Design of an Environmental Stress Cracking (ESC) Tester using Fracture Mechanics Approach

*Muhamad Syafiq Mohamad Nor Azli, Muhammad Faris Mohd Radzi, Muhammad Naguib Ahmad Nazri, Mohd Shahneel Saharudin**
Universiti Kuala Lumpur Malaysia Italy Design Institute (UniKL MIDI), Taman Shamelin Perkasa, Cheras Kuala Lumpur, 56100, MALAYSIA
**mshahneel@unikl.edu.my*

Fawad Inam
Department of Engineering and Computing, University of East London, London E16 2RD, United Kingdom

ABSTRACT

In this research, an ESC tester machine was built by utilising a fracture mechanics approach. The machine consists of critical components such as an aluminium frame, 3D printed pulley and bracket, DC motor, Arduino microcontroller, and fasteners. The test was performed by securing an acrylic sample using a hook fixed to bracket on the base of the frame and integrated load cell with Arduino microcontroller board. Digital camera was used to capture images with Image J processing software to measure the transient damage area and macro-crack length development at each test condition. The results suggested that the applied load can influence the fracture toughness values. At 55N, the fracture toughness for the acrylic was 1.9 MPa.m$^{1/2}$. Increasing the load to 65N, the fracture toughness dropped by 60% to 0.7 MPa.m$^{1/2}$. The minimum fracture toughness was observed at 85N load; a 91% reduction was recorded. Maximum damage area of 89 mm^2 was recorded for sample tested at 55N while minimum damage area was at 85N load, where only 31.81 mm^2 area was calculated. It can be concluded that this newly built machine can be used to perform fracture toughness test on polymeric materials under environmental stress cracking (ESC) condition.

Keywords: *Fracture mechanics, stress cracking, design, image processing, polymer.*

ISSN 1823-5514, eISSN2550-164X
Received for review: 2020-08-14
Accepted for publication: 2020-11-18
Published: 2021-01-15

Introduction

Environmental stress cracking (ESC) is an unexpected brittle failure and has been one of the most common problems for thermoplastic based materials, with an enormous industrial and economic implications [1]. In general, the ESC phenomenon occurs on plastics when polymer-based products are subjected to both mechanical stress and aggressive liquid exposure [2]. However, in certain scenarios, even if amorphous polymers are in contact with non-aggressive liquid like water, the stress failure is also slightly lower than their estimated limit due to plasticization and softening effects. In the past 70 years, the mechanisms of ESC failure in polymeric materials have been widely studied [3, 4]. The development of ESC in plastics was observed to be more of a physical than a chemical process [5, 6]. The aggressive liquid media does not cause a chemical degradation of the polymer, but gradually dispersed into the polymer matrices under tension and causes hydrostatic pressure [7], which expedites the cracking movement and consequently produces unexpected brittle catastrophe of the plastic based components [8]. It has been determined that ESC is accountable for 25% of plastic component failures in service [9, 10] as ESC was observed as one of the most common reasons for the unexpected brittle failure of thermoplastic polymers [11, 12].

The history of ESC test on thermoplastic polymers using fracture mechanics approach can be traced back to 1998 from a publication by Moskala [13]. In this particular publication, a plaque produced from injection moulding technique was machined according to compact tension sample to study creep crack growth rate as a function of K_{1C}. Apart from that, this research also determined polymer molecular weight and studied the effects of caustic concentration on creep crack growth behaviour.

Scanning Electron Microscopy analysis of the fracture surfaces revealed that crack growth proceeded by the formation of novel discontinuous growth bands. In most recent studies by Lin and Schlarb [8] and Nomai et al. [9], these authors also used similar method, however their main contributions were towards the experimental system. They reported on the temporal development of damage area and recorded their results using a Canon CCD-camera. In addition, a constant load of 300 N was applied on all compact tension specimens and all recorded images were saved and analysed for image processing analysis. Damage area and crack length were calculated from the pixel numbers. In order to calculate the pixel numbers, a reference line was drawn on specimens before any experimental work was carried out.

Unexpected brittle failure caused by ESC can be a two-step process; initiation of a crack followed by propagation of the crack until failure. Flaws such as contaminants, impurities, shrinkage voids and machining marks often causes crack initiation. Therefore, crack initiation is more of an erratic process and is hard to measure by means of experimental approach.

Nevertheless, crack propagation can be studied through fracture mechanics approach, in which the crack is located, (da/dt) or known as the rate of crack propagation is recorded as a function of the applied loading and the geometry of the structure. In case of a crack growing is gradual and in stable manner, the relationship between da/dt and K is stated by;

$$da/dt=AK^m \quad (1)$$

where A and m are constants which depend on material properties and test conditions.

The objective of this research is to design and fabricate ESC tester using the fracture mechanics approach. Even though ESC behaviour has been widely discussed in literature, there is no single study which report on the design of ESC tester using fracture mechanics approach. The design and fabrication of inexpensive ESC tester is shown and the manufacturing method of important components were also presented in this report.

Methods

Figure 1 shows the flowchart of the design process. Normally in design process, a flowchart is used to show the steps involved in product development. In this research, the first step was to define the problem with respect to existing design from literature. It is worth to mention that previous studies have not dealt with the design of ESC tester. Most studies only produce 2D drawing of experimental setup and the load applied to their materials. The following step was to determine the design specifications based on requirement needed in the experimental work.

The main components involved were load, motor type, pulley, wire rope, clamping device with an aluminum frame making up as the machine structure. Then, based on these requirements, the conceptual design was presented and designed using CAD software (Solidworks). Prior to that, a simulation of electronics circuit and the coding was performed using Tinkercad software.

Next, complete assembly of all mechanical parts was done in Solidworks to achieve precision and efficiency. Design improvement and optimization of materials were also carried out at this stage. After careful considerations, actual fabrication and assembly were then executed. EDM wire cut was used to cut the aluminum stand for clamping purpose whilst 3D printer was used to manufacture the customized pulley and bracket.

Various fixtures like bolts and nuts, aluminum frame, bearing and pins were acquired from Asia Bolts and Nuts Sdn. Bhd., Kuala Lumpur, Malaysia.

Final testing was carried out to ensure all components were appropriately assembled so that the machine can function as intended.

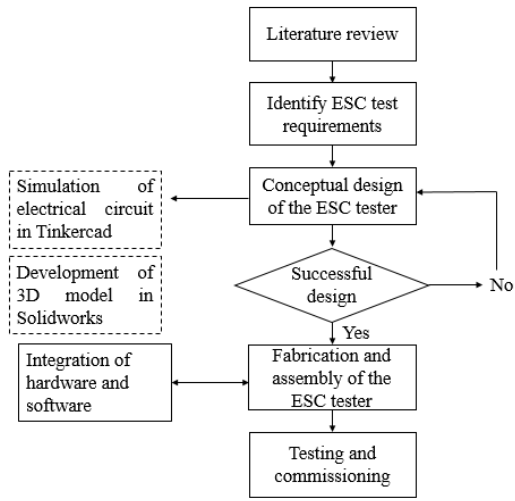

Figure 1: Flowchart of the ESC tester design process.

The schematic of experimental setup in Figure 2 was obtained from the design process and used as guidelines for the conceptual design. Acrylic sheet 3 mm in thickness acquired from Acrylic Signs Material, Off Jalan Pasar, Kuala Lumpur, Malaysia was used as polymer sample.

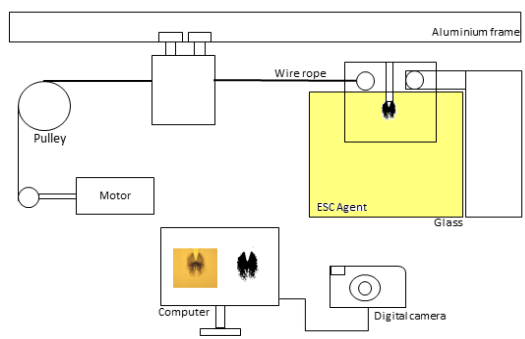

Figure 2: Schematic of experimental setup (not drawn to scale).

Compact tension specimens were cut using laser cutter machine as shown in Figure 3, and the dimensions referred from previous publication is shown in Figure 4 [8, 13, 14].

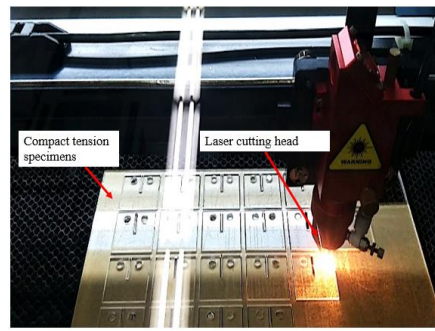

Figure 3: Preparation of compact tension specimens using laser cutter machine.

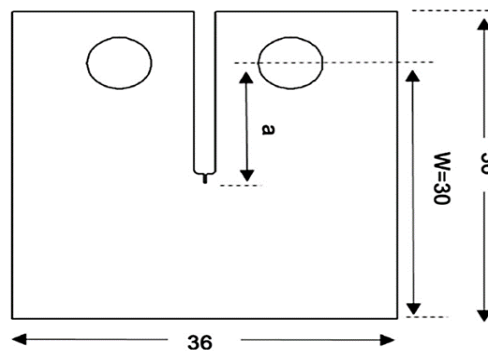

Figure 4: Compact tension sample.

A sharp pre-crack was made by tapping a razor blade into the bottom of the sample slots. The pre-crack length should be between 0.45 to 0.55 mm. The pre-crack device is shown in Figure 5. The sample is then placed at the bottom and razor blade is fitted onto the load container. At pre-determined height, the load is released to produce a pre-crack on compact tension sample. Since this research paper focuses on the design of ESC tester, the design of pre-crack device is not discussed here.

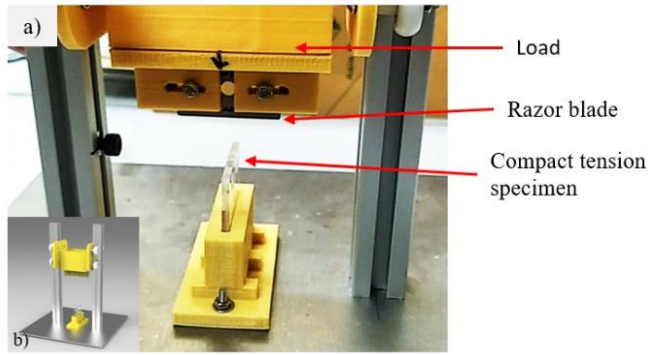

Figure 5: (a) Actual pre-crack station and, (b) a 3D rendering image in Solidworks.

The K_1c was obtained from the following equation.

$$K_{1c} = f\left(\frac{a_0}{W}\right).\left(\frac{F_{max}}{BW^{1/2}}\right) \quad (2)$$

A schematic of the rig used for the crack growth test is shown below. A customized 3D printed pulley is pulled by steel rope 1mm in diameter and attached to an aluminium T-slot to allow for uniaxial translation. The 3D printed pulley and a bracket are shown in Figure 6.

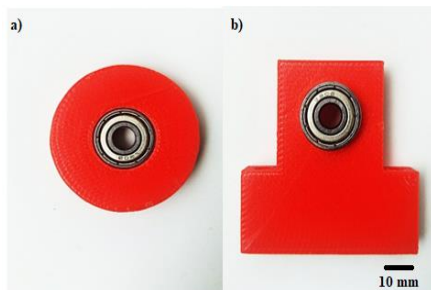

Figure 6: Customized 3D printed parts; pulley (a) and bracket (b) fitted with bearings.

In order to determine the mechanical properties of a sample, applied load and extension were recorded. A micro load cell from luggage scale was used to measure any changes in applied load. The change of crack length was also measured using ultrasonic sensor. Both the load cell and ultrasonic

sensor were connected to Arduino microcontroller. Table 1 shows the list of main components and their prices. The total cost to build this portable machine was RM 1,638.45 and the cost breakdown of each component is as presented.

Table 1: List of main components and prices

No.	List of main component	Purpose	Specifications	Cost (RM)
1	Aluminium T-slot	Frame	45mmx45mm	45.40
2	Pulley with bearing	Support movement and change of direction	Bearing diameter 17 mmx 12 mm	26.00
3	DC Motor	Converts energy from electrical to mechanical	12V	18.00
4	Motor speed controller	Control motor speed	3A, 4-16V	35.00
5	Steel rope/wire	Connects pulley and motor	1 meter length	26.96
6	Load cell	Converts a force into an electrical signal	Maximum load 45kg	24.95
7	Arduino Uno microcontroller	Control operations	Supply voltage 12V Analog input pins 6 SRAM 2kB	40.00
8	Glass container	Contain aggressive liquid	100mmx100mmx100mm	21.00
9	Bolts and nuts	Fastener	M4x50mm M6x50mm	25.00
10	Acrylic	Cover	500x300mmx3mm	60.28
11	Camera	Image capture	EOS 4000D	1250
12	Software	Post processing	ImageJ	0
Total cost				RM 1638.45

Characterization of ESC

The specimens for ESC-testing were prepared as mentioned earlier. The compact tension sample was immersed in the stress cracking agent, methanol. Mechanical properties of a sample were determined based on two parameters; load applied and also the extension. Further crack at the damaged area will completely be surrounded by the methanol during testing period. The time-based development of the crack length and damage area was monitored and recorded using a Canon CCD-camera. A load of 55N, 65N, 75N and 85N were applied to all the test samples. Wire rope was pulled by a motor governed by the speed controller. Load cell was connected to the hook attached to sample. The load can be measured using load cell from luggage scale placed in series with the compact tension sample. Changes in length of sample or simply known as extension was then measured by ultrasonic sensor. The sensor takes all the measurement from the frame to central loading [15]. The measured crack length gave an input to the calculation of K_{1C}. Post processing analysis was then carried out using ImageJ software [16] to determine the transient damage area as well as crack growth size by analysing all the captured surface images that were saved into the computer. The images were initially transformed to a binary image and then the pixels with certain grey level were selected by a defined threshold. Then the damage area was calculated based on the pixel numbers. The wiring configuration from digital Vernier calliper to Arduino microcontroller is shown in Figure 7. Rendered image of the ESC tester is shown in Figure 8(a) and (b). Load cell and ultrasonic sensor that were linked to Arduino Uno microcontroller is also presented in Figure 8(b). The measurement of surface roughness was performed using Mitutoyo surface roughness tester. Five readings were taken and computed at 0.25 mm cut off.

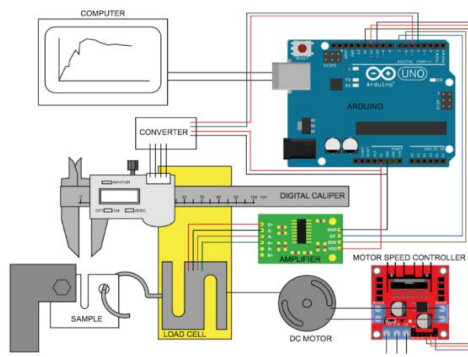

Figure 7: Wiring configuration from digital Vernier calliper to Arduino microcontroller.

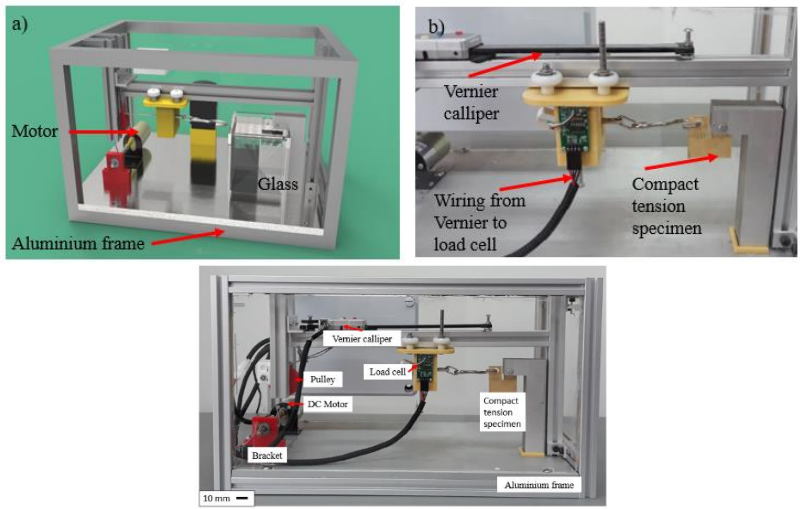

Figure 8: (a) Rendering image of an ESC tester in Solidworks, (b) wiring from Vernier calliper to load cell and front view of actual ESC tester

Results and discussion

Figure 9 shows initial sample setup in Smart Shooter remote capture and advanced camera control mode. The images were captured in video format with frame rate of 40 fps. FPS is also known as the frequency at which consecutive images called frames appearing on a display. Figure 10 shows the development of crack as a function of time. It can be observed that the crack developed really quick when aggressive liquid like methanol is in contact with polymeric material subjected to stress. We have tested four different loads on the acrylic samples to determine the differences among them and validate the machine. Figure 11 shows how the damage area was determined. First, the image was converted to grayscale by converting each pixel's colour information into a brightness measurement. In the ImageJ toolbar, a rectangle was used to specify the area of interest. Then, based on known reference line, the area was calculated. The result shows that the fracture toughness of acrylic samples depends on the applied load. The higher the load, the lower the fracture toughness. Figure 12 (a) shows at 55N load, the fracture toughness for acrylic sample was 1.9 $MPa.m^{1/2}$. When the load was increased to 65N, the fracture toughness dropped 60% to 0.7 $MPa.m^{1/2}$. Likewise, the minimum fracture toughness was observed at 85N load, where a 91% reduction was recorded. It was also noted that the results

presented here were in line with existing publication by Lin and Schlarb where a critical fracture toughness K_{1C} for neat polycarbonate was approximately 5 MPa.m$^{1/2}$ [8]. The difference in K_{1C} is due to the different material types. We believe that this mechanical tester is an ideal tool for ESC test. The damage areas calculated from grey scale images were presented in Figure 12 (b). Sample tested at 55N load obtained the highest damage area (89 mm^2), and this can be associated with the high fracture toughness. The higher the fracture toughness, the longer will be the immersion time and damage area. The minimum damage area was observed for sample tested with 85N load, where 32 mm^2 in damage area was recorded. Low fracture toughness means the sample failed rapidly and the immersion time is shorter than sample with higher fracture toughness. The effect of ESC agent on the surface roughness is presented in Figure 12(c). The measurement was carried out using portable Mitutoyo surface roughness tester on immersed samples. The results indicate that the highest surface roughness was observed for sample tested with 55N, where the roughness was 4.7 µm. Sample tested with 85N load recorded only 0.4 µm roughness value.

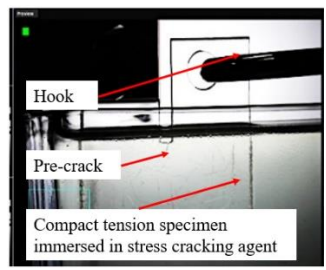

Figure 9: Initial sample setup in remote capture and advanced camera control.

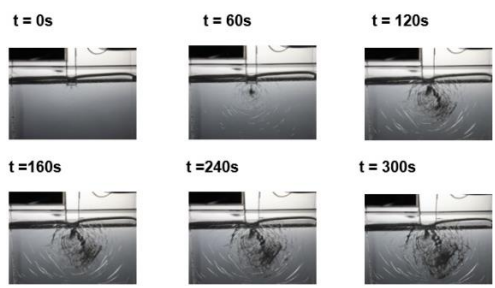

Figure 10: Development of crack as a function of time.

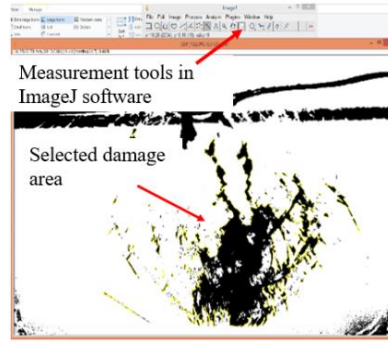

Figure 11: Selected damage area calculation in ImageJ software.

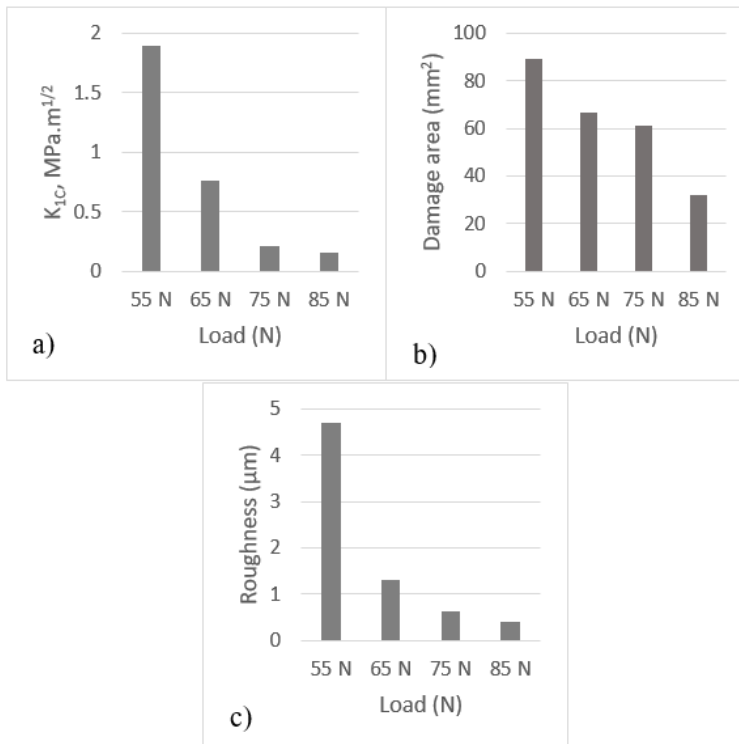

Figure 12: (a) K_{1C} of acrylic at different loads, (b) damage area of acrylic at different loads, and (c) effect of ESC agent on acrylic surface roughness.

Conclusion

In this project an ESC tester using fracture mechanics approach was successfully designed and fabricated. The total cost of this project is RM 1,638. The results show that at 55N load, the fracture toughness for acrylic sample was 1.9 MPa.$m^{1/2}$. In the case of 65N load, the fracture toughness dropped 60% to 0.7 MPa.$m^{1/2}$. Likewise, the minimum fracture toughness was observed at 85N load, where a 91% reduction was recorded. The damage area calculated from grey scale images also indicated similar trend. Sample tested at 55N load resulted in the highest damage area (89 mm^2), this can be associated with the high fracture toughness. The higher the fracture toughness, the longer is the immersion time and damage area. The minimum damage area was observed for sample tested with 85N load, where 32 mm^2indamage area was recorded. Low fracture toughness means that the sample failed rapidly and the immersion time is shorter than sample with higher fracture toughness. The effect of ESC agent on the surface roughness was also studied. The results show that the highest surface roughness was observed in sample tested with 55N load, where the roughness was 4.7 µm. Sample tested with 85N load recorded only 0.4 µm roughness value. The surface roughness values were aligned with fracture toughness results presented earlier. It can be concluded that this machine can be used to measure fracture toughness of polymeric based materials. However, a contact between the liquid used in this experimental work and load cell could damage the component. Thus, this can be the limitation of the developed ESC tester. A customised lid can be fabricated and placed on top of glass to reduce risk of spillage. For future recommendation, the ESC tester can be improved by replacing wire rope and pulley with an electrical powered screw mechanism. In this way, the load can be equally distributed and the deformation of wire rope can be avoided.

Acknowledgement

The authors would like to thank the Centre for Research & Innovation (CORI) Universiti Kuala Lumpur for the financial support, without which the analysis of relevant data will not be possible.

References

[1] C. Hopmann, N. Borchmann, S. Koch, and D. Alperstein, “Influencing the environmental stress cracking resistance of amorphous thermoplastic parts by the example of polycarbonate and water,” *Polym. Eng. Sci.*, vol. 59, no. S1, pp E361-E366, 2019.

[2] L. F. Al-Saidi, K. Mortensen, and K. Almdal, “Environmental stress

cracking resistance. Behaviour of polycarbonate in different chemicals by determination of the time-dependence of stress at constant strains," *Polym. Degrad. Stab.*, vol. 82, no. 3, pp 451–461, 2003.

[3] A. K. Saad, H. A. Abdulhussain, F. P. C. Gomes, J. Vlachopoulos, and M. R. Thompson, "Studying the mechanism of biodiesel acting as an environmental stress cracking agent with polyethylenes," *Polymer (Guildf).*, vol. 191, pp 122278, 2020.

[4] P. R. Lewis, "Environmental stress cracking of polycarbonate catheter connectors," *Eng. Fail. Anal.*, vol. 16, no. 6, pp 1816–1824, 2009.

[5] R. F. Farias, E. L. Canedo, R. M. R. Wellen, and M. S. Rabello, "Environmental Stress Cracking of Poly (3-hydroxibutyrate) Under Contact with Sodium Hydroxide 3," *Mater. Res.*, vol. 18, no. 2, pp 258–266, 2015.

[6] M. Khodabandelou, M. K. Razavi Aghjeh, and M. Rezaei, "Fracture behavior and environmental stress cracking resistance (ESCR) of HIPS/PE blends and the effect of compatibilization on their properties," *Eng. Fract. Mech.*, vol. 76, no. 18, pp 2856–2867, 2009.

[7] M. S. Saharudin, A. Rasheed, I. Shyha, and F. Inam, "The degradation of mechanical properties in halloysite nanoclay – polyester nanocomposites exposed to diluted methanol," *Journal of Composite Materials*, vol. 51, no. 11, pp 1653-1664, 2017.

[8] L. Lin and A. Schlarb, "A study on environmental stress cracking in nano-SiO2-filled polycarbonate," *J. Mater. Sci.*, vol. 47, no. 18, pp 6614–6620, 2012.

[9] J. Nomai and A. K. Schlarb, "Environmental stress cracking (ESC) resistance of polycarbonate/SiO_2 nanocomposites in different media," *Journal of Applied Polymer Science*, vol. 134, no. 43, pp 45451, 2017.

[10] L. M. Robeson, "Environmental stress cracking: A review," *Polym. Eng. Sci.*, vol. 53, no. 3, pp 453–467, 2013.

[11] M. S. Saharudin, R. Atif, I. Shyha, and F. Inam, "The degradation of mechanical properties in polymer nano-composites exposed to liquid media – a review," *RSC Adv.*, vol. 6, no. 2, pp 1076–1089, 2016.

[12] L. Andena, L. Castellani, A. Castiglioni, A. Mendogni, M. Rink, and F. Sacchetti, "Determination of environmental stress cracking resistance of polymers: Effects of loading history and testing configuration," *Eng. Fract. Mech.*, vol. 101, pp 33–46, 2013.

[13] E. J. Moskala, "A fracture mechanics approach to environmental stress cracking in poly(ethyleneterephthalate)," *Polymer (Guildf).*, vol. 39, no. 3, pp 675–680, 1998.

[14] M. S. Saharudin, J. Wei, I. Shyha, and F. Inam, "Environmental Stress Cracking Resistance of Halloysite Nanoclay-Polyester Nanocomposites," *World J. Eng. Technol.*, vol. 5, no. 3, pp 389–403, 2017.

[15] J. H. Arrizabalaga, A. D. Simmons, and M. U. Nollert, "Fabrication of an Economical Arduino-Based Uniaxial Tensile Tester," *J. Chem. Educ.*, vol. 94, no. 4, pp 530–533, 2017.
[16] E. Moghbelli, R. Banyay, and H.-J. Sue, "Effect of moisture exposure on scratch resistance of PMMA," *Tribol. Int.*, vol. 69, pp 46–51, 2014.